Hindawi
International Journal of Polymer Science
Volume 2017, Article ID 8745405, 12 pages
https://doi.org/10.1155/2017/8745405

Research Article

Effect of Bolt-Hole Clearance on Bolted Connection Behavior for Pultruded Fiber-Reinforced Polymer Structural Plastic Members

Sang-Pyuk Woo,[1] Sun-Hee Kim,[2] Soon-Jong Yoon,[1] and Wonchang Choi[2]

[1] *Department of Civil Engineering, Hongik University, Seoul 04066, Republic of Korea*
[2] *Department of Architectural Engineering, Gachon University, 1342 Seongnam-daero, Sujeong-gu, Seongnam-si, Gyeonggi-do 13120, Republic of Korea*

Correspondence should be addressed to Wonchang Choi; wonchang.choi@gmail.com

Received 11 March 2017; Revised 22 May 2017; Accepted 5 July 2017; Published 6 August 2017

Academic Editor: Reza Aliha

Bolt-hole clearance affects the failure mode on the bolted connection system of pultruded fiber-reinforced polymer plastic (PFRP) members. The various geometric parameters, such as the shape and cross-sectional area of the structural members, commonly reported in many references were used to validate the bolt-hole clearance. This study investigates the effects of the bolt-hole clearance in single-bolt connections of PFRP structural members. Single-bolt connection tests were planned using different bolt-hole clearances (e.g., tight-fit and clearances of 0.5 mm to 3.0 mm with 0.5 mm intervals) and uniaxial tension is applied on the test specimens. Most of the specimens failed in two sequential failure modes: bearing failure occurred and the shear-out failure followed. Test results on the bolt-hole clearances are compared with results in the previous research.

1. Introduction

Until the 1990s, the use of fiber-reinforced polymer plastic (PFRP) composites was limited to aerospace and military applications [1]. However, the fiber-reinforced plastic (FRP) composites have many advantageous mechanical properties, such as an excellent strength-to-weight ratio and stiffness-to-weight ratio, which make them highly desirable also as a building material for civil engineering applications [2, 3]. Therefore, efforts to include FRP materials in civil engineering have been increased markedly over recent decades. In order to use FRP materials in the construction field, the pultruded structural member must be connected. Several types of connections are currently used for this purpose, including bolted, bonded, a combination of bolted and bonded, and interlocking connections. For civil engineering applications, bolted connections are preferred and deemed the most practical because they are easy to assemble and disassemble, easy to maintain, and are usually cost-effective when compared with the other types of connections [4].

In general, there are four possible failure modes for pultruded fiber-reinforced polymer plastic (PFRP) single-bolted connections that are subjected to tensile forces [5–12], as shown in Figure 1. Figure 1(a) illustrates net-tension failure, which is attributable to the reduced cross-sectional area of a FRP member that is due to the bolt hole. Figure 1(b) shows cleavage-tension failure where the cross-sectional area of the bolt is not resistant to tensile loading and breaks away from the contact point. Figures 1(c) and 1(d) show bearing failure and shear-out failure, respectively.

Conventionally, FRP materials are failed in a brittle mode [12], whereas bearing failure allows ductile behavior unlike the other failure modes (net-tension failure, cleavage-tension failure, and shear-out failure). Bearing failure is the most likely to occur when FRP material is used in a structural member. Various parameters need to be taken into account to ensure safety in the design with regard to the bolt connection in order to induce bearing failure. Researchers and manufacturers who have studied bolt connections of composite materials have suggested a geometric recommendation index based on experiments and experience [16–24]. Geometric

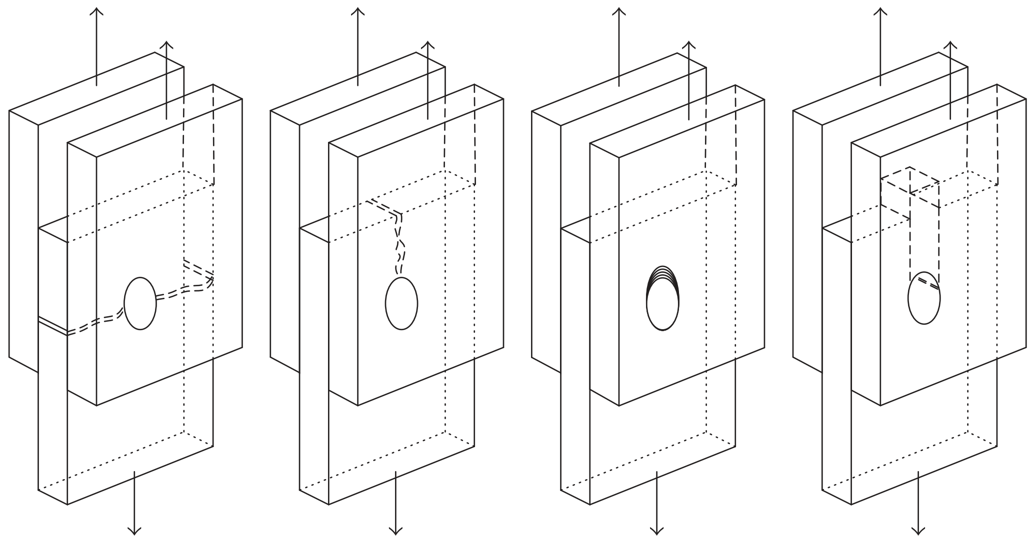

(a) Net-tension failure (b) Cleavage-tension failure (c) Bearing failure (d) Shear-out failure

Figure 1: Typical failure modes of bolted connections.

coefficients for a bolt's width-to-diameter ratio of 6 (i.e., $w/d = 6$) and end-to-diameter ratio of 3 (i.e., $e/d = 3$) were proposed to induce bearing failure according to ASTM Standard D5961/D5961 M-96 [21]. Rosner and Rizkalla [6] reported that bearing failure mode occurs predominantly with an increase in the use of high geometric coefficient values for both the width-to-diameter ratio and end-to-diameter ratio. They recommended that the geometric coefficients (w/d and e/d) should be greater than 5.0. Therefore, the geometric coefficients used in this study are $w/d = 5$ and $e/d = 5$.

The clearance between the bolt diameter (d_b) and the hole diameter (d_h) is one of the parameters that allows constructability and ductile failure in the bolt connection. However, very few experiments have been conducted with regard to the necessary clearance, and existing codes recommend various values to determine the appropriate bolt-hole clearance. Thus, this study aims to address this informational deficit and determine the adequate bolt-hole clearance to prevent brittle failure in a single-bolted connection system for PFRP materials. A total of 98 single-bolt connection specimens with various bolt-hole clearances were tested under tensile loading. Also, the existing available code values found in the Eurocomp Design Code [13] and the Italian National Research Council (CNR) standards [14] and the bolt-hole clearance reported by Mottram [15] were compared with the experimental results obtained.

2. Experimental Program

2.1. Mechanical Properties of PFRP Structural Members. Two shapes, angle, and I-shape, of PFRP structural members were investigated. The PFRP structural members were fabricated in Korea using the pultrusion process and manufactured using E-glass fiber and polyester resin with the fiber volume fraction of 0.578. In the pultruded structural shapes, E-glass fiber bundles are placed along the longitudinal direction of the member.

Figure 2 presents the dimensions of two types of PFRP specimens.

The material properties of the PFRP members were determined from tensile tests, compression tests, and shear tests. The tensile test specimens were taken in the longitudinal direction (i.e., the member axis direction that coincided with the reinforcing fiber direction) and prepared, with slight modification, according to ASTM D3039/D3039 M-08 [26]. Figure 3 shows the prismatic tensile test specimens and test setup. Fifteen specimens were prepared, including five specimens from the angle (specimen dimension: 250.00 × 24.78 × 9.82 mm) and ten specimens from the I-shape (specimen dimension: 250.00 × 25.44 × 9.62 mm). Each specimen was loaded up to failure with a loading speed of 3 mm/min in accordance with the displacement control method. In these tensile tests, all the specimens are failed in a brittle manner within the gage length.

In order to determine the modulus of elasticity along the transverse direction of each specimen, tensile strength test specimens should be taken along the transverse direction of the member to comply with ASTM D3410/D3410 M-03. However, in this study, the compressive strength test, instead of tensile test, suggested by Yoon [27] was adopted because taking a tension test specimen in the transverse direction of the member [28] is not possible because the width of flange and web are too small. Figure 4 shows the compression specimens and test setup used in this study. Fifteen specimens were prepared, including five specimens from the angle of structural member (specimen dimension: 80.00 × 19.79 × 9.83 mm) and ten specimens from the I-shape (specimen dimension: 80.00 × 18.29 × 9.50 mm). Each specimen was loaded up to failure with a loading speed of 3 mm/min

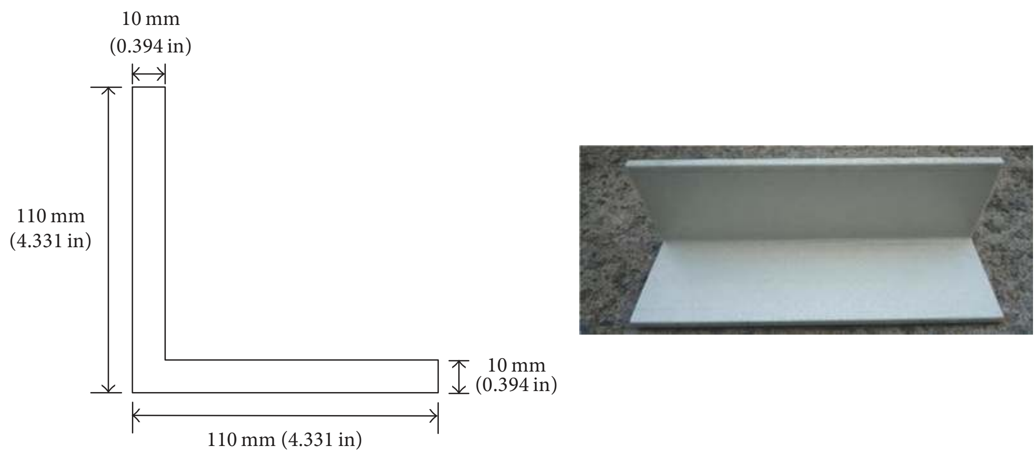

(a) Angle

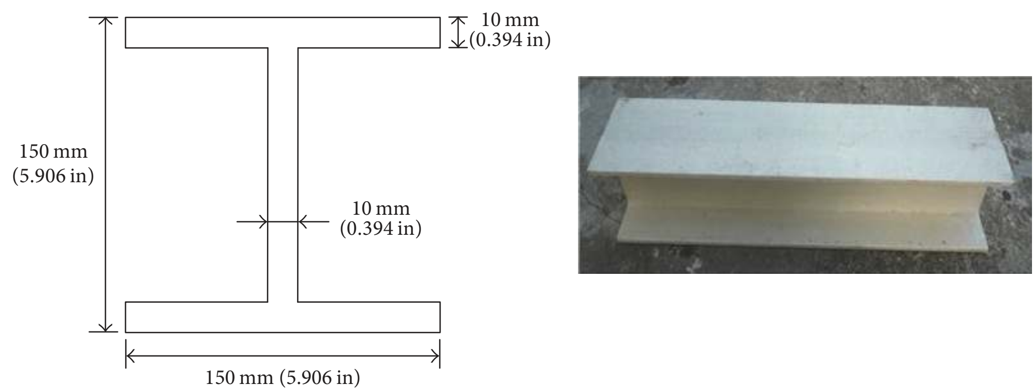

(b) I-shape

Figure 2: Structural shape and its cross-section dimension.

Table 1: Mechanical properties of PFRP members.

Test	PFRP member		Average strength (MPa)	Average modulus of elasticity (GPa)	Number of specimens
Tensile	Angle		524.32 ± 25.10	35.12 ± 8.87	5
	I-shape		415.31 ± 86.45	32.65 ± 3.33	10
Compression	Angle		147.32 ± 7.38	13.24 ± 1.67	5
	I-shape		161.91 ± 9.01	12.31 ± 2.84	10
Shear	Angle	Axial	87.31 ± 3.80	6.30 ± 0.97	5
		Transverse	61.28 ± 4.83	6.01 ± 0.58	5
	I-shape	Axial	76.30 ± 4.17	5.40 ± 0.68	10
		Transverse	41.41 ± 6.77	6.33 ± 1.97	10

according to the displacement control method. In these compressive tests, all the specimens are failed in a brittle manner within the gage length.

Finally, shear tests for the PFRP specimens were also conducted according to the method found in ASTM D5379/D5379 M-12 [29]. Figure 5 shows a shear test specimen and test setup. Thirty specimens were prepared, including 10 specimens from the angle type (specimen dimension: 76.27 × 12.06 × 9.22 mm) of structural member in both the longitudinal direction and transverse directions and 20 specimens from the I-shape type (specimen dimension: 76.01 × 12.04 × 12.20 mm) also in the longitudinal and transverse directions. Load was applied with a speed of 1.27 mm/min according to the displacement control method.

Table 1 presents a summary of the average test results for the three types of tests performed in terms of the specimens' mechanical properties.

2.2. Single-Bolted Connections. The connection specimens tested in this investigation consisted of rectangular plates that

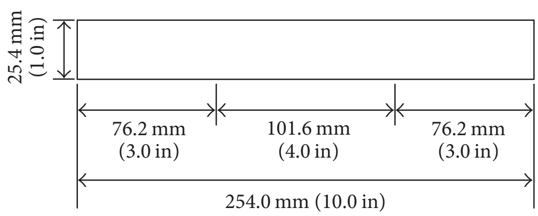

(a) Specimen dimension

(b) Tensile test specimens

(c) Test setup

(d) Failed specimen

Figure 3: Tensile test specimens and test setup.

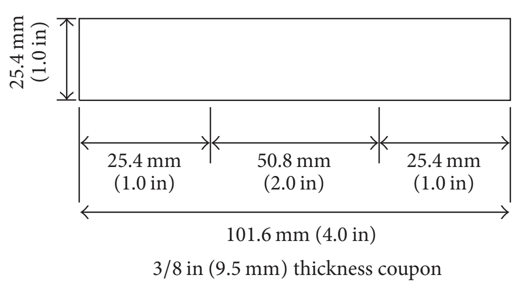

(a) Specimen dimension

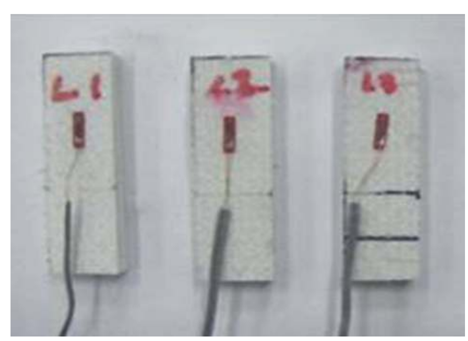

(b) Compressive test specimens

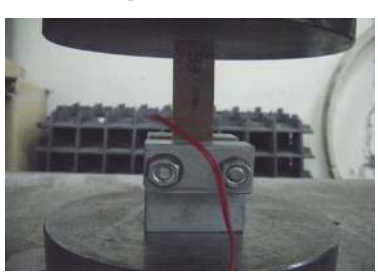

(c) Test setup

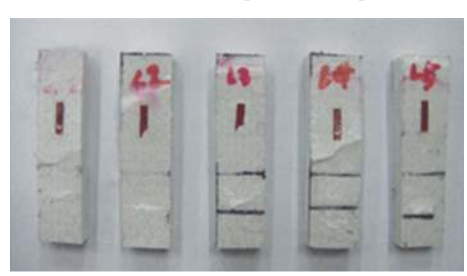

(d) Failed specimen

Figure 4: Compression test specimens and test setup.

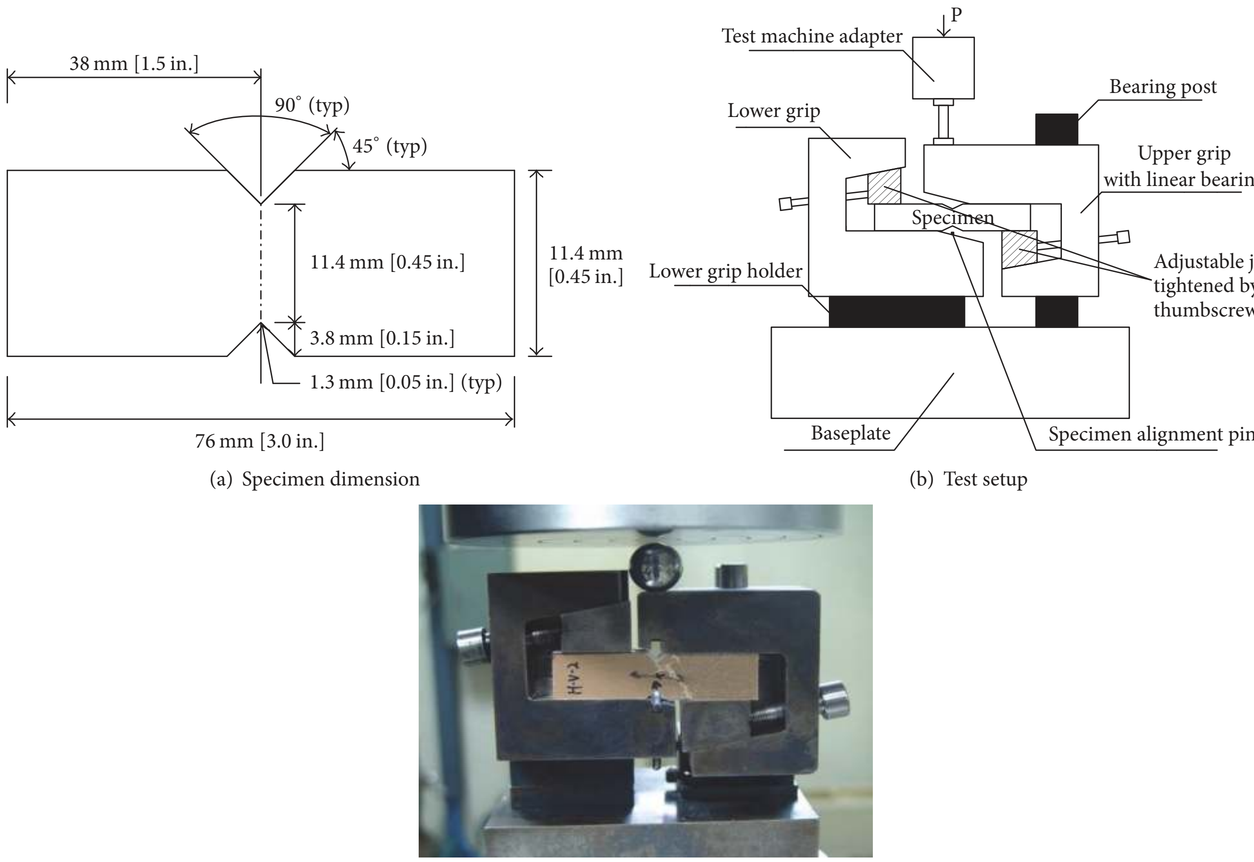

(a) Specimen dimension

(b) Test setup

(c) Failed specimen

Figure 5: Shear test specimen and test setup.

were cut from two types of PFRP structural members (angle and I-shape) using a table-saw with a diamond-tipped blade. At one end of each plate, holes were marked and drilled the desired end distance according to the specified pattern for the connection. Rectangular plates for I-shape-1, I-shape-2, and I-shape-3 were cut from the flange and web of I-shape PFRP member. Table 2 provides detailed dimensions of the single-bolted test specimens. A total of 98 bolted connection specimens (i.e., angle and I-shape-3 specimens: three for each test variation, I-shape-1, and I-shape-2 specimens: four for each test variation) were prepared by drilling holes with different bolt-hole clearances. The specimens identified with a member shape, bolt diameter, and bolt-hole clearance.

Stainless steel hexagon head screws (M10) [30], stainless steel hexagon nuts (M10) [31], and stainless steel plain washers [32] were used in the fabrication of the connection test specimens that were taken from the angle and I-shape-1 structural members. Steel hexagon head bolts (M10, M12) [30], steel hexagon head nuts (M10, M12) [31], and stainless steel plain washers [32] were also used in the fabrication of the connection test specimens taken from the I-shape-2 and I-shape-3 specimens. Figures 6 and 7 describe the geometric parameters for the single-bolted connections and the three types of bolts (including nuts and washers) used in the test, respectively.

Four basic geometric parameters that may affect the strength and the failure mode of single-bolt connections were investigated in the experimental program: the width of the member (w), the end distance (e), the hole clearance ($d_h - d_b$), and the reinforcing fiber direction of the PFRP structural shapes (refer to Figure 6). Rosner and Rizkalla [6] reported that the thickness (t) of the specimen barely affects the experimental results in overlapped spliced joint tests; thus, the dimensions specified by the manufacturer were used without any further process.

2.3. Tension Tests for Single-Bolted Connections. Tension tests using single-bolted connections were conducted using a 1000-kN Universal Testing Machine. Figure 8 presents the tension test for a double-lapped joint and the test setup. The grip plates were made using a stainless steel plate. Also, a stainless steel hexagon head screw (M10) and steel hexagon head bolt (M10, M12) were used to fabricate the connection test system. Tensile loading was applied with a displacement rate of 1 mm/min (0.167 mm/sec) in accordance with ASTM D953-10 [33].

3. Test Results and Discussion

3.1. Tension Test Results for Single-Bolted Connections. As shown in Figure 9, local failure load is defined as the load

Table 2: Dimensions of test specimens connected with a single-bolt.

Shape	Specimen designation	Geometric parameter (mm)					e/d_b	w/d_b	d_b/t	$d_h - d_b$	Number of specimens
		e	w	t	d_b	d_h					
Angle	A-C0.0	50	50	10	10	10	5	5	1	0	3
	A-C0.5					10.5				0.5	3
	A-C1.0					11				1.0	3
	A-C1.5					11.5				1.5	3
	A-C2.0					12				2.0	3
	A-C2.5					12.5				2.5	3
	A-C3.0					13				3.0	3
I-shape-1	I-C0.0	50	50	10	10	10	5	5	1	0	4
	I-C0.5					10.5				0.5	4
	I-C1.0					11				1.0	4
	I-C1.5					11.5				1.5	4
	I-C2.0					12				2.0	4
	I-C2.5					12.5				2.5	4
	I-C3.0					13				3.0	4
I-shape-2	I-B10-C0.0	50	50	10	10	10	5	5	1	0	4
	I-B10-C0.5					10.5				0.5	4
	I-B10-C1.0					11.0				1.0	4
	I-B10-C1.5					11.5				1.5	4
	I-B10-C2.0					12.0				2.0	4
	I-B10-C2.5					12.5				2.5	4
	I-B10-C3.0					13				3.0	4
I-shape-3	I-B12-C0.0	50	50	10	12	12	4.17	4.17	1.2	0	3
	I-B12-C0.5					12.5				0.5	3
	I-B12-C1.0					13				1.0	3
	I-B12-C1.5					13.5				1.5	3
	I-B12-C2.0					14				2.0	3
	I-B12-C2.5					14.5				2.5	3
	I-B12-C3.0					15				3.0	3

at which the bearing failure mode changes to the shear-out failure mode. The load-displacement curves for the specimens indicate a local failure load after which the load increases and then decreases slightly and continuously up to the point where the structural fracture load is reached.

Figures 10 and 11 show the failure modes at each stage of load increment. Table 3 presents a summary of the local failure loads, structural fracture loads, and corresponding modes of failure for all the tested connection specimens for the two structural profile sections used in this investigation. In Table 3, the failure modes are described as CT (cleavage-tension), B (bearing), and S (shear-out). There is no net-tension failure (NT) in this study.

3.2. Effects of Bolt-Hole Clearance. For civil engineering applications, maintaining a uniform and precise size for the bolt-hole clearance is important for constructability. Table 4 shows the bolt-hole clearance suggested in the Eurocomp Design Code [13], the Italian National Research Council (CNR) standard [14], and previous research [15].

To investigate the effects of variation in the bolt-hole clearances, the failure loads were plotted with respect to the bolt-hole clearances ($d_h - d_b$), as shown in Figures 12–15.

Figures 12–14 shows no noticeable trend in the changes in the structural fracture load with respect to the bolt-hole clearance. In contrast, a significant decreasing trend is evident in the results for the local failure load. Therefore, the difference between the local failure load and the structural fracture load is larger if the bolt-hole clearance has increased. However, Figure 15 shows that the structural fracture load for I-shape-3 with respect to the bolt-hole clearance has a decreasing trend.

In previous research [34], coupon tests were conducted using the whole cross-section of pultruded I-shape specimens. A total of 18 coupons were cut from the cross-section: six coupons from the upper flange, six coupons from the

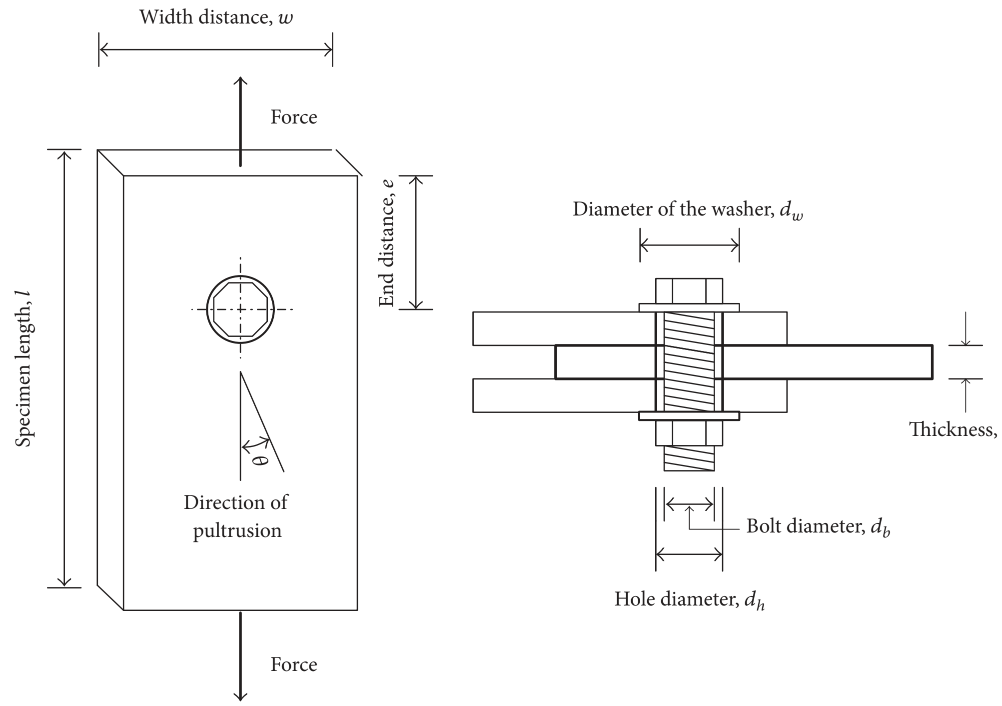

Figure 6: Geometric parameters for single-bolted connections.

(a) Stainless steel hexagon head screw (M10)
(b) Steel hexagon head bolt (M10)
(c) Steel hexagon head bolt (M12)

Figure 7: Type of bolt, nut, and washer used in the test.

lower flange, and six coupons from the web. The results for the material property variation tests show that the longitudinal elastic modulus is different in the range of 9 percent to 23 percent. This variation of the elastic modulus may affect the failure load of the specimen.

The reinforcing fiber direction and sampling location in the structural shape produced by the pultrusion process may result in differences between the elastic moduli of the web and flange of the PFRP structural shapes. Therefore, the structural fracture load decreased slightly. Similarly, the discrepancy between the local failure load and structural fracture load increased with an increase in the bolt-hole clearance.

A relatively large bolt-hole clearance is preferred for easy of fabrication of the structure to secure constructability. The recommended value suggested in the Eurocomp Design Code [13] seems to be too small to use in practice. In addition, the application of the Eurocomp simplified method for the design of bolted joints for PFRP materials is questionable because of its reliance on single-curve normalized stress distributions. The CNR standard [14] proposes a bolt-hole clearance of 1 mm. However, because the time required for the structural fracture load to occur after the local failure load test is too short, the test specimen is not suitable for use as a design basis in consideration to safety. Therefore, the suggested bolt-hole clearance of 1.6 mm (1/16 in.) found in the Mottram [15] is preferable because this clearance dimension accounts for the span between the local failure point (which is the ductile failure mode) and the structural failure point (which is the fracture point), even if the FRP is a brittle material. The ASCE Design Guide for FRP Composite Connections [24]

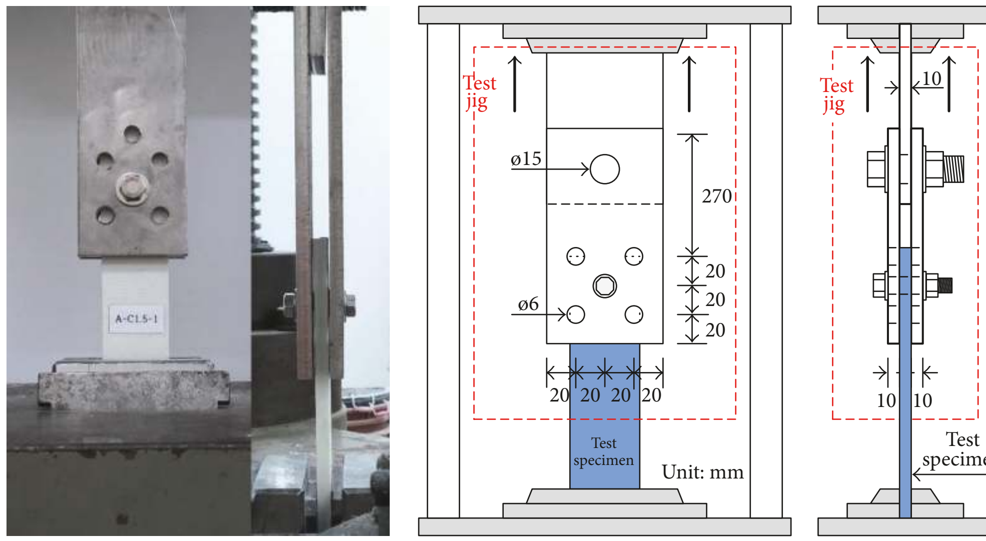

Figure 8: Tension test setup for a single-bolted connection [25].

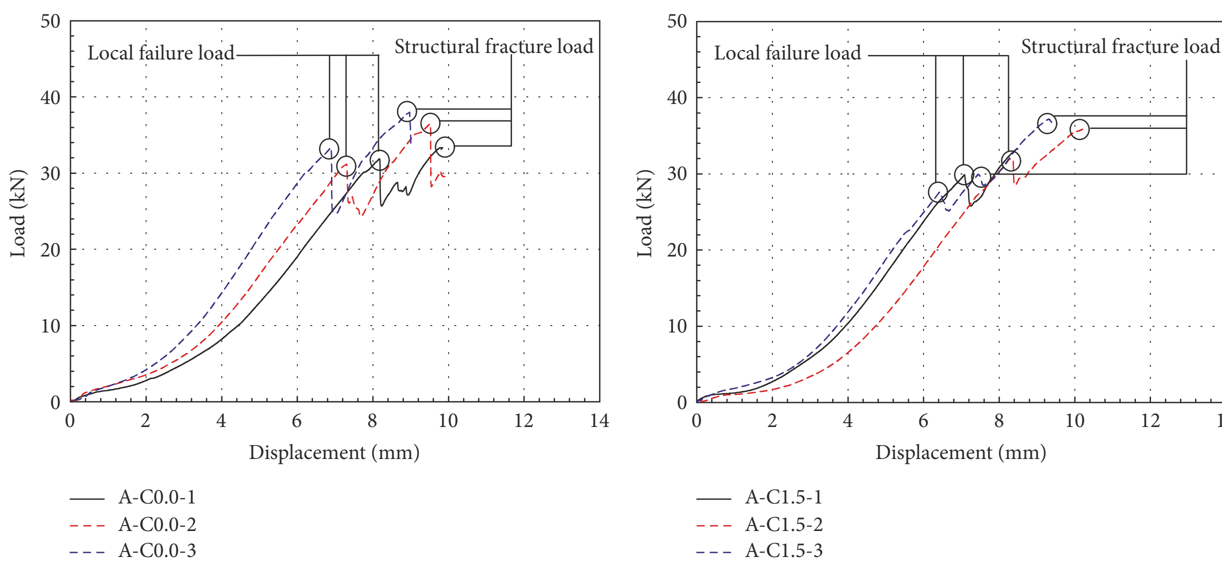

(a) Three specimens for A-C0.0

(b) Three specimens for A-C1.5

Figure 9: Relationship between load and displacement.

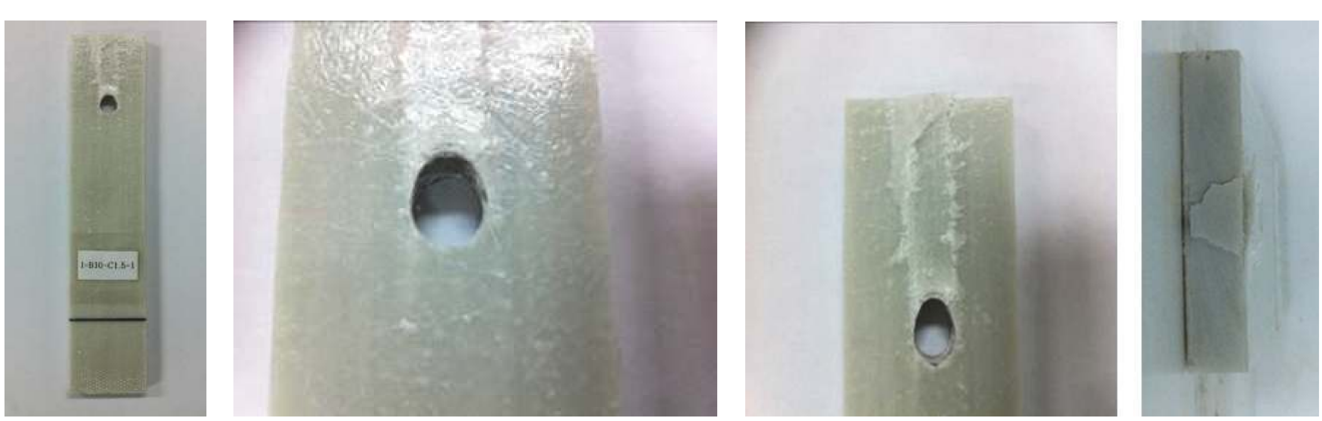

(a) Failed specimen

(b) Local failure mode (bearing failure)

(c) Structural fracture mode (shear-out failure)

Figure 10: Examples of local failure and structural fracture modes (I-B10-C1.5 specimen).

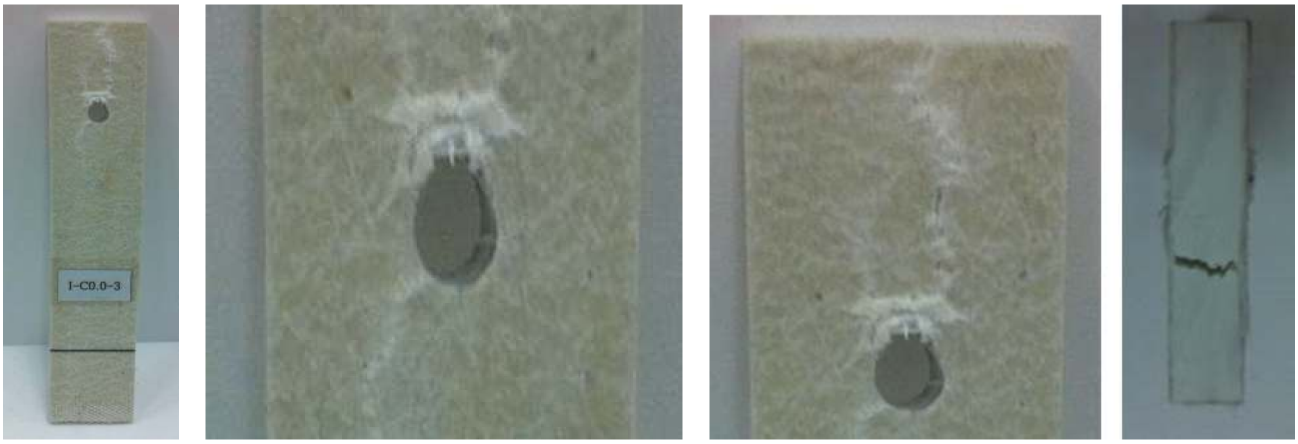

(a) Failed specimen (b) Local failure mode (bearing failure) (c) Structural fracture mode (cleavage-tension failure)

Figure 11: Examples of local failure and structural fracture modes (I-C0.0 specimen).

Table 3: Experimental results for PFRP bolted connections.

Shape	ID	e/d_b	w/d_b	d_b/t	$d_h - d_b$	Average local failure load (kN)	Local failure mode	Average structural fracture load (kN)	Structural fracture mode
	A-C0.0				0	32.25 ± 1.00	B	35.97 ± 2.43	S
	A-C0.5				0.5	28.59 ± 2.74	B	38.26 ± 1.02	S
	A-C1.0				1.0	29.00 ± 3.15	B	38.56 ± 3.68	S
Angle	A-C1.5	5	5	1	1.5	29.81 ± 2.19	B	35.44 ± 1.98	S
	A-C2.0				2.0	29.64 ± 1.81	B	35.95 ± 2.77	S
	A-C2.5				2.5	25.37 ± 3.38	B	38.65 ± 2.28	S
	A-C3.0				3.0	24.63 ± 1.05	B	37.19 ± 2.28	S
	I-C0.0				0	30.63 ± 3.64	B	30.77 ± 3.93	CT
	I-C0.5				0.5	27.81 ± 1.83	B	30.45 ± 3.32	S
	I-C1.0				1.0	27.79 ± 2.79	B	28.96 ± 3.25	S
I-shape-1	I-C1.5	5	5	1	1.5	27.66 ± 3.44	B	29.54 ± 2.04	S
	I-C2.0				2.0	25.66 ± 1.78	B	27.96 ± 2.62	S
	I-C2.5				2.5	25.37 ± 4.34	B	30.69 ± 2.28	S
	I-C3.0				3.0	27.19 ± 2.87	B	30.62 ± 3.56	S
	I-B10-C0.0				0	29.73 ± 0.57	B	30.07 ± 0.92	S
	I-B10-C0.5				0.5	23.83 ± 5.13	B	30.47 ± 1.51	S
	I-B10-C1.0				1.0	23.68 ± 4.70	B	29.69 ± 0.69	S
I-shape-2	I-B10-C1.5	5	5	1	1.5	20.95 ± 7.73	B	26.65 ± 3.55	S
	I-B10-C2.0				2.0	18.43 ± 4.45	B	29.06 ± 4.27	S
	I-B10-C2.5				2.5	22.41 ± 5.36	B	29.31 ± 1.77	S
	I-B10-C3.0				3.0	24.12 ± 2.27	B	28.72 ± 3.57	S
	I-B12-C0.0				0	34.13 ± 0.12	B	34.40 ± 0.53	CT
	I-B12-C0.5				0.5	25.73 ± 8.70	B	32.40 ± 2.96	S
	I-B12-C1.0				1.0	33.13 ± 0.61	B	34.87 ± 2.95	S
I-shape-3	I-B12-C1.5	4.17	4.17	1.2	1.5	31.13 ± 3.44	B	32.93 ± 1.36	S
	I-B12-C2.0				2.0	24.20 ± 0.92	B	32.07 ± 3.51	S
	I-B12-C2.5				2.5	19.00 ± 6.94	B	26.67 ± 6.80	S
	I-B12-C3.0				3.0	25.67 ± 3.25	B	30.07 ± 2.20	S

Note. Although all of the specimens were assumed to have exact sizes for bolt-hole clearance, however, in practice some error in clearance size was unavoidable during the specimen preparation and testing, which may affect the test results.

Table 4: Recommended bolt-hole clearance.

Reference	Eurocomp [13]	Italian CNR [14]	Mottram [15]
Bolt hole clearance	Tight fit ($0.05d_b$)	≤1 mm	1/16 in (1.6 mm)

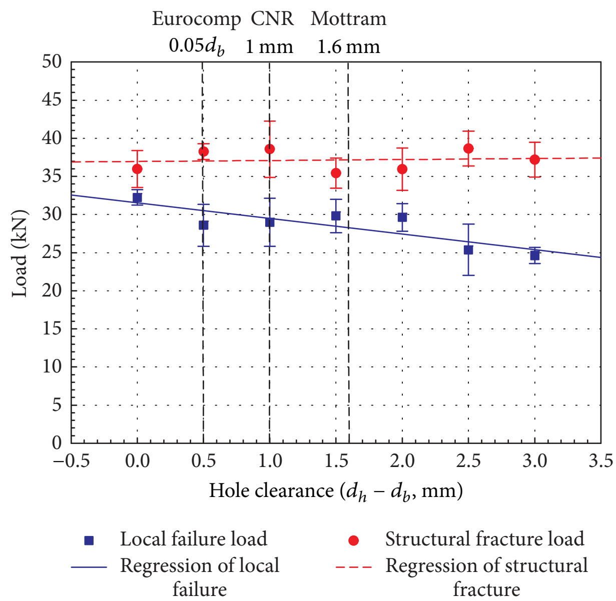

Figure 12: Relationship between load and bolt-hole clearance (specimen from angle).

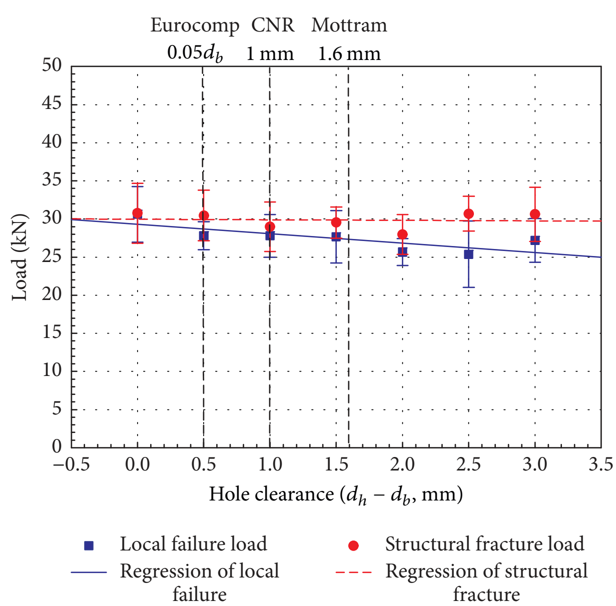

Figure 13: Relationship between load and bolt-hole clearance (specimen from I-shape-1).

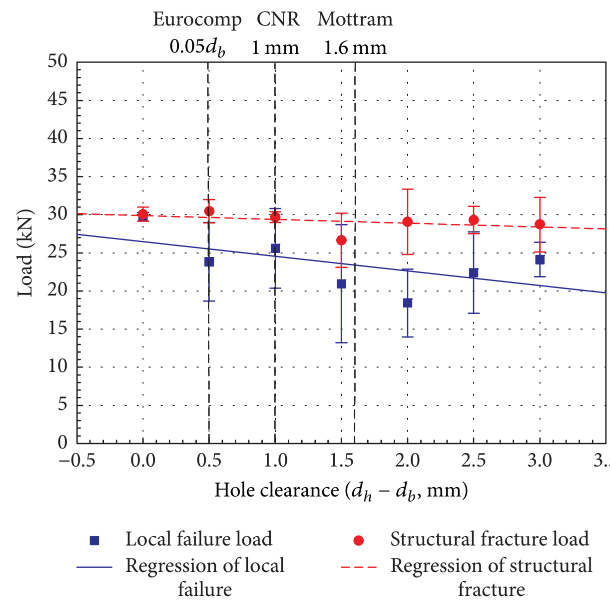

Figure 14: Relationship between load and bolt-hole clearance (specimen from I-shape-2).

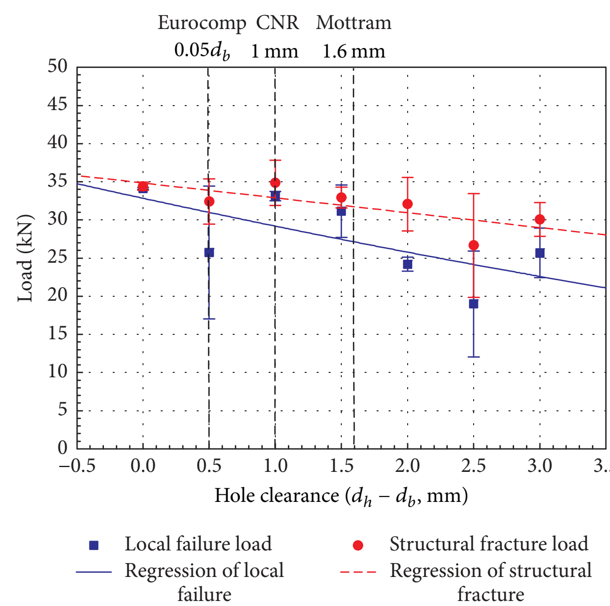

Figure 15: Relationship between load and bolt-hole clearance (specimen from I-shape-3).

was discussed on the effect of bolt fit (hole clearance). The hole diameter, d, equals the bolt diameter, d_b, plus 5/8 in. (15.875 mm) which may acceptable in practice. However, it is felt that 15.875 mm hole clearance is too large to be efficient to induce bearing failure mode.

4. Conclusions

In this paper we investigated the effects of bolt-hole clearance in single-bolted connections in the PFRP structural members. Different sizes of bolt-hole clearance from tight-fit to 3.0 mm with 0.5 mm intervals were investigated. The experimental results in terms of local failure load, structural fracture load, and failure mode were analyzed with respect to the geometric parameters (i.e., the bolt-hole clearances). The following results were found.

(1) The specimens, in general, failed with two sequential failure modes. The bearing failure mode appeared first and the shear-out failure mode followed. Therefore, the geometric parameters of the specimens, that is, the e/d and w/d, were needed to maintain with sufficient values regardless of the bolt-hole clearance. For each case, bearing failure was the predominant failure mode.

(2) When the bolt-hole clearances were in the range of 0 mm to 3 mm, no significant trend was evident with regard to the structural fracture loads. However, the local failure load decreased if the bolt-hole clearance was increased. Differences between the structural fracture loads and the local failure loads were greater when the bolt-hole clearance was increased.

(3) Constructability can be ensured by maintaining a minimum bolt-hole clearance. The Eurocomp Design Code recommends a bolt-hole clearance that is ($d_h - d_b$) $0.05d_b$ (5%) of the bolt diameter, but this recommended clearance may be not efficient in practice.

(4) The recommended bolt-hole clearances found in both the Eurocomp and CNR standards are not suitable in terms of safety due to the small interval from the local failure load to the structural fracture load. The bolt-hole clearance of 1.6 mm (1/16 in.) found in the previous research [15] is appropriate and allows ductile failure.

Conflicts of Interest

The authors declare that there are no conflicts of interest regarding the publication of this paper.

Acknowledgments

This work was supported by the Energy Research & Development of the Korea Institute of Energy Technology Evaluation and Planning (KETEP) grant funded by the Korean Government's Ministry of Trade, Industry & Energy (no. 20161120200190).

References

[1] L. Feo, G. Marra, and A. S. Mosallam, "Stress analysis of multi-bolted joints for FRP pultruded composite structures," *Composite Structures*, vol. 94, no. 12, pp. 3769–3780, 2012.

[2] M. C. Wang, *Connection capacity of pultruded gfrp channels in multidirectional loading [M.S. Thesis]*, University of Colorado, 2013.

[3] M. Shokrieh and M. Heidari-rarani, "Experimental and analytical studies on one-way concrete slabs reinforced with GFRP molded gratings," *Steel and Composite Structures*, vol. 9, no. 6, pp. 569–584, 2009.

[4] CN. Rosner, *Single-bolted connections for orthotropic fibre-reinforced composite structural members [M. S.Thesis]*, University of Manitoba, 1992.

[5] B. Vangrimde and R. Boukhili, "Descriptive relationships between bearing response and macroscopic damage in GRP bolted joints," *Composites Part B: Engineering*, vol. 34, no. 7, pp. 593–605, 2003.

[6] C. N. Rosner and S. H. Rizkalla, "Bolted connections for fiber-reinforced composite structuralmembers: Experimental program," *Journal of Materials in Civil Engineering*, vol. 7, no. 4, pp. 223–231, 1995.

[7] S. F. M. Abd-El-Naby and L. Hollaway, "The experimental behaviour of bolted joints in pultruded glass/ polyester material. Part 1: Single-bolt joints," *Composites*, vol. 24, no. 7, pp. 531–538, 1993.

[8] C. Cooper and G. J. Turvey, "Effects of joint geometry and bolt torque on the structural performance of single bolt tension joints in pultruded GRP sheet material," *Composite Structures*, vol. 32, no. 1-4, pp. 217–226, 1995.

[9] G. J. Turvey, "Single-bolt tension joint tests on pultruded GRP plate - effects of tension direction relative to pultrusion direction," *Composite Structures*, vol. 42, no. 4, pp. 341–351, 1998.

[10] Ü. Esendemir, "An experimental study of mechanically fastened composite joints with clearance," *International Journal of Damage Mechanics*, vol. 20, no. 3, pp. 464–480, 2011.

[11] F. Sen, M. Pakdil, O. Sayman, and S. Benli, "Experimental failure analysis of mechanically fastened joints with clearance in composite laminates under preload," *Materials & Design*, vol. 29, no. 6, pp. 1159–1169, 2008.

[12] J. T. Mottram and G. J. Turvey, "Physical test data for the appraisal of design procedures for bolted joints in pultruded FRP structural shapes and systems," *Progress in Structural Engineering and Materials*, vol. 5, no. 4, pp. 195–222, 2003.

[13] *Eurocomp Design Code and Handbook. Structural Design of Polymer Composites*, The European Structural Polymeric Composites Group, 1996.

[14] Technical Document, "Guide for the Design and Construction of Structures Made of FRP Pultruded Elements," Tech. Rep. CNR-DT 205/2007, Italian National Research Council (CNR), Rome, Italy, 2008.

[15] J. T. Mottram, "Design guidance for bolted connections in structures of pultruded shapes: gaps in knowledge," in *Proceedings of the 4th International Conference on Advanced Composites in Construction (ACIC 2009)*, pp. 483–495, NetComposites Ltd, Chesterfield, UK, 2009.

[16] V. P. Lawlor, M. A. McCarthy, and W. F. Stanley, "An experimental study of bolt-hole clearance effects in double-lap, multi-bolt composite joints," *Composite Structures*, vol. 71, no. 2, pp. 176–190, 2005.

[17] T. A. D. Tajeuna, F. Légeron, S. Langlois, P. Labossière, and M. Demers, "Effect of geometric parameters on the behavior of bolted GFRP pultruded plates," *Journal of Composite Materials*, vol. 50, no. 26, pp. 3731–3749, 2016.

[18] Y. Xiao and T. Ishikawa, "Bearing strength and failure behavior of bolted composite joints (part I: Experimental investigation)," *Composites Science and Technology*, vol. 65, no. 7-8, pp. 1022–1031, 2005.

[19] G. Kelly and S. Hallström, "Bearing strength of carbon fibre/epoxy laminates: Effects of bolt-hole clearance," *Composites Part B: Engineering*, vol. 35, no. 4, pp. 331–343, 2004.

[20] M. A. McCarthy, V. P. Lawlor, W. F. Stanley, and C. T. McCarthy, "Bolt-hole clearance effects and strength criteria in single-bolt, single-lap, composite bolted joints," *Composites Science and Technology*, vol. 62, no. 10-11, pp. 1415–1431, 2002.

[21] ASTM, "Standard test method for bearing response of polymer matrix composite laminates," ASTM International 5961/D 5961 M-05, West Conshohocken, PA, USA, 2005.

[22] F. Ascione, L. Feo, and F. Maceri, "An experimental investigation on the bearing failure load of glass fibre/epoxy laminates," *Composites Part B: Engineering*, vol. 40, no. 3, pp. 197–205, 2009.

[23] A. A. Pisano, P. Fuschi, and D. De Domenico, "A layered limit analysis of pinned-joints composite laminates: Numerical versus experimental findings," *Composites Part B: Engineering*, vol. 43, no. 3, pp. 940–952, 2012.

[24] A. S. Mosallam, "Design for FRP composite connections," *ASCE Manuals and Reports on Engineering Practice*, 2011.

[25] Y.-G. Lee, E. Choi, and S.-J. Yoon, "Effect of geometric parameters on the mechanical behavior of PFRP single bolted connection," *Composites Part B: Engineering*, vol. 75, pp. 1–10, 2015.

[26] ASTM, "Standard test method for tensile properties of polymer matrix composite materials," ASTM International 3039/D 3039 M-08, West Conshohocken, PA, USA, 2008.

[27] S. J. Yoon, *Local buckling of pultruded I-shape columns [Ph.D. thesis]*, Georgia Institute of Techonlogy, Atlanta, GA, USA.

[28] Y. G. Lee, J. S. Park, J. H. Nam, D. J. An, and S-J. Yoon, "Structural behavior of PFRP connection with single bolt," in *Proceedings of the 18th International Conference on Composite Materials (ICCM' 18)*, pp. 1–5, Jeju Island, Korea, August 2011.

[29] ASTM, "Standard test method for shear properties of composite materials by the V-notched beam method," ASTM International D 5379/D 5379 M-12, West Conshohocken, PA, USA, 2012.

[30] KS B 1002. Hexagon Head Bolts and Hexagon Head Screws. Korea: Korean Standards Association, 2001.

[31] KS B 1012. Hexagon Nuts and Hexagon Thin Nuts. Korea: Korean Standards Association, 2001.

[32] KS B 1326. Plain Washers. Korea: Korean Standards Association, 2009.

[33] ASTM, "Standard test method for bearing strength of plastics," ASTM International D 953-10, West Conshohocken, PA, USA, 2010.

[34] H. Choi, J. W. Choi, H. J. Joo, D. J. An, and S-J. Yoon, "Effects of material properties variations on the local buckling loads of pultruded structural shapes," *Journal of Computational Design and Engineering*, vol. 1, pp. 645–648, 2009.